Earthq Eng & Eng Vib (2017) 16: 447-458 **DOI**: 10.1007/s11803-017-0392-y

Soil characterization of Tınaztepe region (İzmir/Turkey) using surface wave methods and nakamura (HVSR) technique

Eren Pamuk[1†], Özkan Cevdet Özdağ[2†], Şenol Özyalın[1‡], Mustafa Akgün[1§]

1. *Dokuz Eylül University Engineering Faculty Department of Geophysical Engineering, İzmir 35160, Turkey*

2. *Dokuz Eylül University Aegean Implementation and Research Center, İzmir 35430, Turkey*

Abstract: To determine the shear wave velocity structure and predominant period features of Tınaztepe in İzmir, Turkey, where new building sites have been planned, active–passive surface wave methods and single-station microtremor measurements are used, as well as surface acquisition techniques, including the multichannel analysis of surface waves (MASW), refraction microtremor (ReMi), and the spatial autocorrelation method (SPAC), to pinpoint shallow and deep shear wave velocity. For engineering bedrock (V_s > 760 m/s) conditions at a depth of 30 m, an average seismic shear wave velocity in the upper 30 m of soil (AV_s30) is not only accepted as an important parameter for defining ground behavior during earthquakes, but a primary parameter in the geotechnical analysis for areas to be classified by V_{s30} according to the National Earthquake Hazards Reduction Program (NEHRP). It is also determined that Z1.0, which represents a depth to V_s = 1000 m/s, is used for ground motion prediction and changed from 0 to 54 m. The sediment–engineering bedrock structure for Tınaztepe that was obtained shows engineering bedrock no deeper than 30 m. When compared, the depth of engineering bedrock and dominant period map and geology are generally compatible.

Keywords: shear wave velocity (V_s), predominant period, engineering bedrock, İzmir

1 Introduction

Located within the Turkish Earthquake Code's first-degree earthquake zone (2007), İzmir is a highly active region in terms of seismicity. As seismic waves pass through the soil's layers on engineering bedrock, their frequency and amplitude change, which is often a primary source of structural damage during earthquakes. Parameters causing such changes include the firmness and depth of engineering bedrock, as well as the V_s values, density, and thickness of layers constituting the ground. To analyze and identify those parameters, any building site's engineering bedrock should be scrutinized and firmly defined, the geological unit that could be bedrock identified, and the layer's firmness and depth from the ground surface analyzed (Akgün *et al*., 2013).

In designing earthquake-resistant structures, the lateral acceleration of earthquakes on the ground surface and the shape of the spectrum are crucial. The soil transfer function should be calculated when defining the lateral acceleration on the ground surface, which involves using the parameters of S-wave velocity, density, and thickness of the ground and the firmness of engineering bedrock. In current earthquake regulations, a depth of 30 m constitutes a basis for defining the ground; beyond that depth, either engineering bedrock has been reached or the dynamic structure of the ground does not change.

In research on engineering bedrock, levels exceeding V_s > 760 m/s are generally defined as engineering bedrock. In order for that definition to be valid, however, S-wave velocity should be no less than 760 m/s below that level (Anbazhagan and Sitharam, 2009). Vertical profiles comprising the S-wave velocity, thickness, and density of layers located up to the depth with the conditions related are accepted as the ground profile. To make the ground and engineering bedrock fully compatible with ground amplification, both an S-wave velocity of >760 m/s should be examined and the S-wave velocity, thickness, and density of layers that constitute the ground profile determined. Accordingly, the soil transfer function used in designing earthquake-resistant structures can be defined thanks to onsite measurements.

To determine S-wave velocity based on the ground profile up to engineering bedrock in the vertical direction, researchers should use geophysical methods appropriate for the study area. To directly obtain the profile of engineering bedrock and S-wave velocity in such research, surface waves, either actively or passively sourced, should be used and V_{s30} values for soil classification defined according to NEHRP (1997).

At present, improved analytical methods originating

Correspondence to: Eren Pamuk, Dokuz Eylül University Engineering Faculty Department of Geophysical Engineering, İzmir 35160, Turkey
Tel: +90 232 3017275; Fax: +90 232 4538366
E-mail: eren.pamuk@deu.edu.tr
†PhD candidate; ‡Assistant Professor; §Professor
Received January 17, 2016; **Accepted** September 13, 2016

from surface waves are used extensively to sidestep problems in other seismic methods such as seismic refraction and seismic reflection (Park *et al*., 1999; Liu *et al*., 2000; Louie, 2001; Okada, 2003). Analytical methods originating from surface waves can be classified into two groups—namely, active source (e.g., multichannel analysis of surface waves, MASW) and passive source (e.g., refraction microtremor, ReMi, and spatial autocorrelation, SPAC)—both of which are widespread given their usefulness in urban areas and low cost. Generally, the aim of these methods is to determine the dispersion curve, since dispersion curve analysis of surface waves can generate profiles of shear wave velocity. The methods have been used by numerous researchers (Tokimatsu *et al*., 1992; Bettig *et al*., 2001; Ohori *et al*., 2002; Okada, 2003; Morikawa *et al*., 2004; Park and Miller, 2005; Chávez–García *et al*., 2005; Chávez–García *et al*., 2006; Kanlı *et al*., 2006, Köhler *et al*., 2007; Pamuk *et al*., 2014).

At the same time, other researchers have used Nakamura's method for soil characterization involving soil resonance frequency (Lermo and Chávez–García, 1993, 1994; Lachet and Bard, 1994; Gitterman *et al*., 1996; Bard, 1998; Konno and Ohmachi, 1998; Mucciarelli, 1998; Dikmen and Mirzaoğlu, 2005; Asten, 2006; Akkaya, 2015).

The aim of this study is to determine soil characterizations that indicate shear wave velocity structure and predominant period features in Tınaztepe, an area of İzmir (Fig. 1). In the study area in İzmir, soil characterization with both active and passive surface wave methods and, using Nakamura's method, the predominant period was identified in the range of 0.05–0.2 s, which indicates that the area exhibits lower predominant periods and less sediment thickness. Using shear wave velocities, engineering bedrock depth was mapped as three-dimensional and shown to be approximately 30 m: between 0–5 m in the northeast, southeast, and northwest parts of the study area, and 30 m in the southwest. Ultimately, V_{s30} values of 420–960

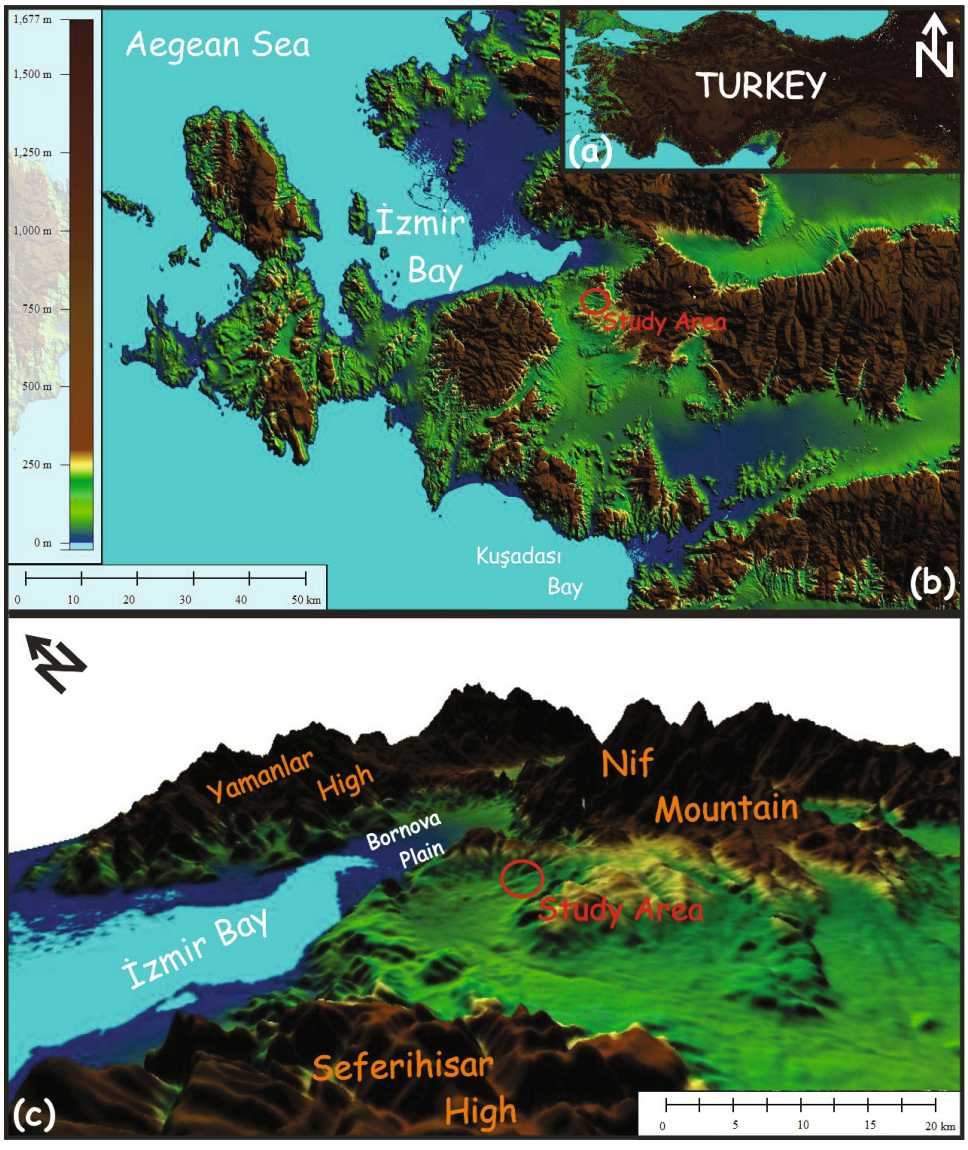

Fig. 1 Site location map of the study area together with general morphology and uplift systems (Yamanlar high, Nif Dağı high and Seferihisar high)

m/s were compatible with the geology and engineering bedrock depth. A cross-section from prepared contour maps was selected and profiles of *S*-wave velocity were interpreted via topography, which showed highly compatible V_s values and deep drilling data. Figure 2 shows a tectonic map of the study area, its environment, and the earthquake activity of the region during 2005–2015 based on the homogenized seismicity catalog recorded during 2005–2015 at the Kandilli Observatory and Earthquake Research Institute's Regional Earthquake-Tsunami Monitoring Center (KOERI (2015)) at Boğaziçi University in İstanbul, Turkey.

The study area and its surroundings had a possible active seismic regime between 2005 and 2015. The region contains many faults, which may cause a major earthquake (Fig. 2). It is inevitable that a study area located in an active tectonic system will experience frequent earthquakes of various magnitudes. This is verified when the seismicity of the region is analyzed. For these reasons, determination of soil characteristics becomes extremely significant for the study area.

2 Geology of the study area

Located in western Turkey on the enlargement of the Western Anatolia tectonic plate, İzmir is a coastal city where many rivers meet the sea and where especially intensive sediment areas occur along the coast. The area studied here is in the southern İzmir Gulf and surrounded by Mount Nif to the east. As Fig. 3 shows, Neogene sedimentary rocks containing fissured limestone–claystone–clayey limestone alternately overlay the Bornova complex (i.e., Bornova mélange, Bornova Flysch Zone) without conformity, and units on the base can be observed from the top-down in the study area and its immediate vicinity (Uzel *et al*., 2012). According to the generalized engineering bedrock model for the study area defined by Özdağ *et al*. (2015), the Bornova mélange is probably engineering bedrock for İzmir Bay and the surrounding area.

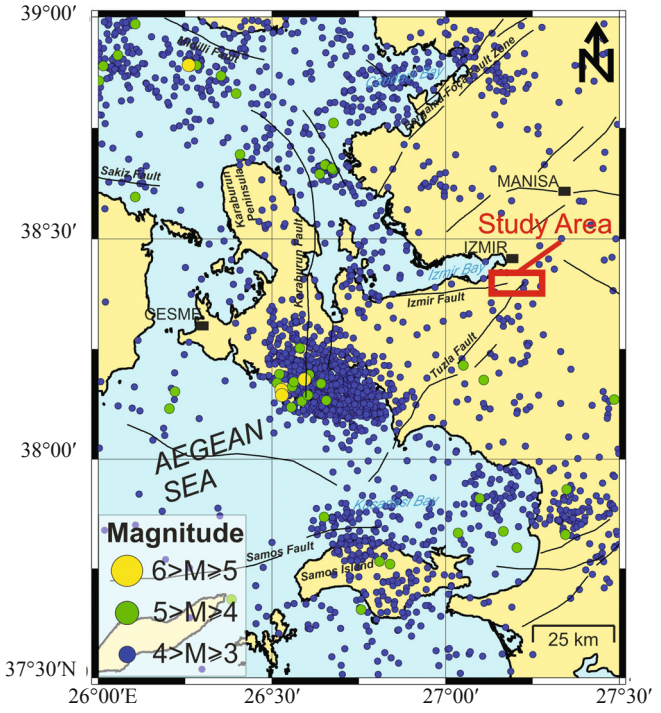

Fig. 2 Tectonic map of study area and its environment and the earthquake activity of the region between 2005 and 2015

3 Methodology

To characterize the soil, the *S*-wave velocity profile was determined from surface waves by using MASW and ReMi, which employs the dispersive properties of Rayleigh waves to image subsurface layers (Park *et al*., 1999; Louie, 2001). As part of Nakamura's method, which is widely used to assess the effect of soil conditions on earthquake shaking, the *H/V* spectral ratio introduced by Nogoshi and Igarashi (1970) was used, which is convenient and inexpensive for soil investigations. Nakamura's method is based on a theory developed by Nakamura (1989), who demonstrated that the ratio between the horizontal and vertical ambient noise records related to the fundamental frequency of the soil beneath a site. The spatial autocorrelation method (SPAC) first proposed by Aki (1957) for horizontally propagating waves was also used to determine deeper V_s profiles.

4 Data acquisition and data analysis

The geophysical site characterization has been utilized in Tınaztepe region in the Buca district of the city of İzmir. MASW (11 sites), ReMi (9 sites), single station microtremor (28 sites) and SPAC (4 sites) measurements were carried out in this study area (Fig. 4).

Within 1 km^2 of the study area, 11 one-dimensional (1-D) MASW measurements were utilized. A MASW system, consisting of a 24-channel Geode seismograph with 24 geophones of 4.5 Hz were used. The seismic waves are generated by impulse source of a hydraulic sledgehammer or a sledgehammer with three shots. Seisimager/SW software was used for analysis of the MASW data. This software contains three-steps for data processing. The first step is preparation of a multichannel record, the second is dispersion curve analysis and the third is inversion (using least-squares approach) (Fig. 5).

Also, nine ReMi measurements were carried out at the same location as the MASW were measurements. The recording time was 30 s for one record. For the ReMi measurements, 12–21 records were recorded at each site. The array lengths were 46 m (two profiles), 115 m (three

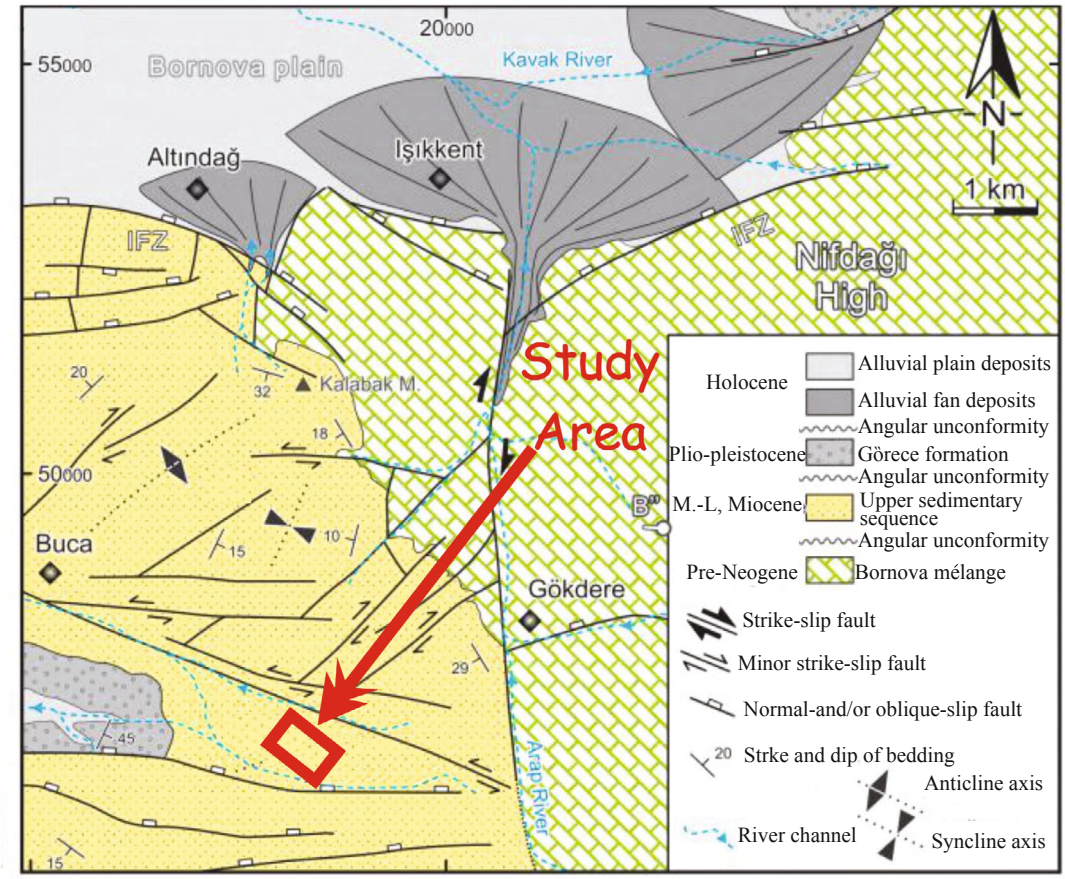

Fig. 3 Geological map of study area (modified from Uzel *et al*., 2012)

Fig. 4 Map of the study area with the locations of the 28 sites of the microtremor measurements and 11 sites of V_s measurements

profiles), 57.7 m (three profiles) and 235 m (one profile). The ReMi interpretation and analysis were carried out using Seisimager/SW software. Data processing of The ReMi consisted of three steps: 1)Velocity spectral (*p-f*) analysis, 2)Rayleigh phase-velocity dispersion picking, 3)Shear wave velocity modeling (Louie, 2001). The graphic representation of the data proccesing steps is shown in Fig. 6.

Microtremor observations were carried out at more than 28 sites in the study area. All of the study area′s Microtremor measurements were taken with the Guralp Systems CMG-6TD seismometer. At each location, the recording duration was 20–30 minutes with a sampling rate of 100 Hz. The records were viewed using the Scream 4.5 program. To remove intensive artificial disturbance in data processing, all signals were filtered in

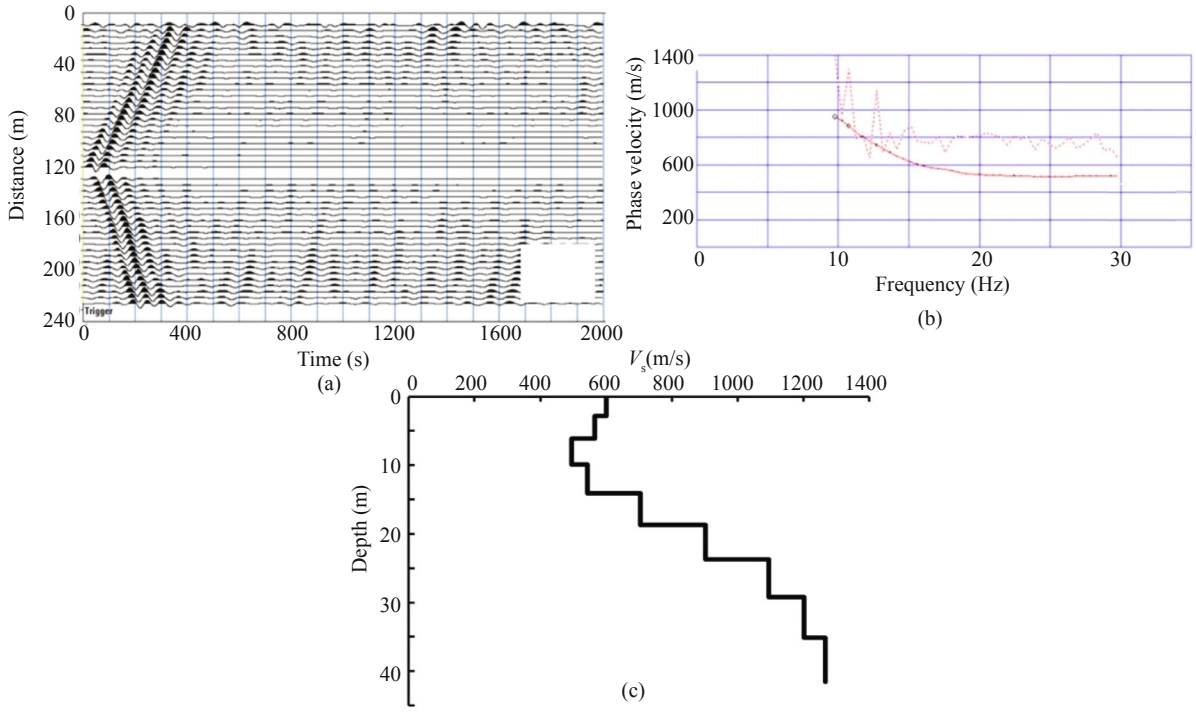

Fig. 5 Data processing steps of MASW data in Site P1: (a) Middle shot record; (b) Determining the phase velocity of each frequency (Dotted red line shows that signal/noise ratio, Continuous red line shows that determined fundamental mode dispersion curve); (c) Shear wave velocity (V_s) profile

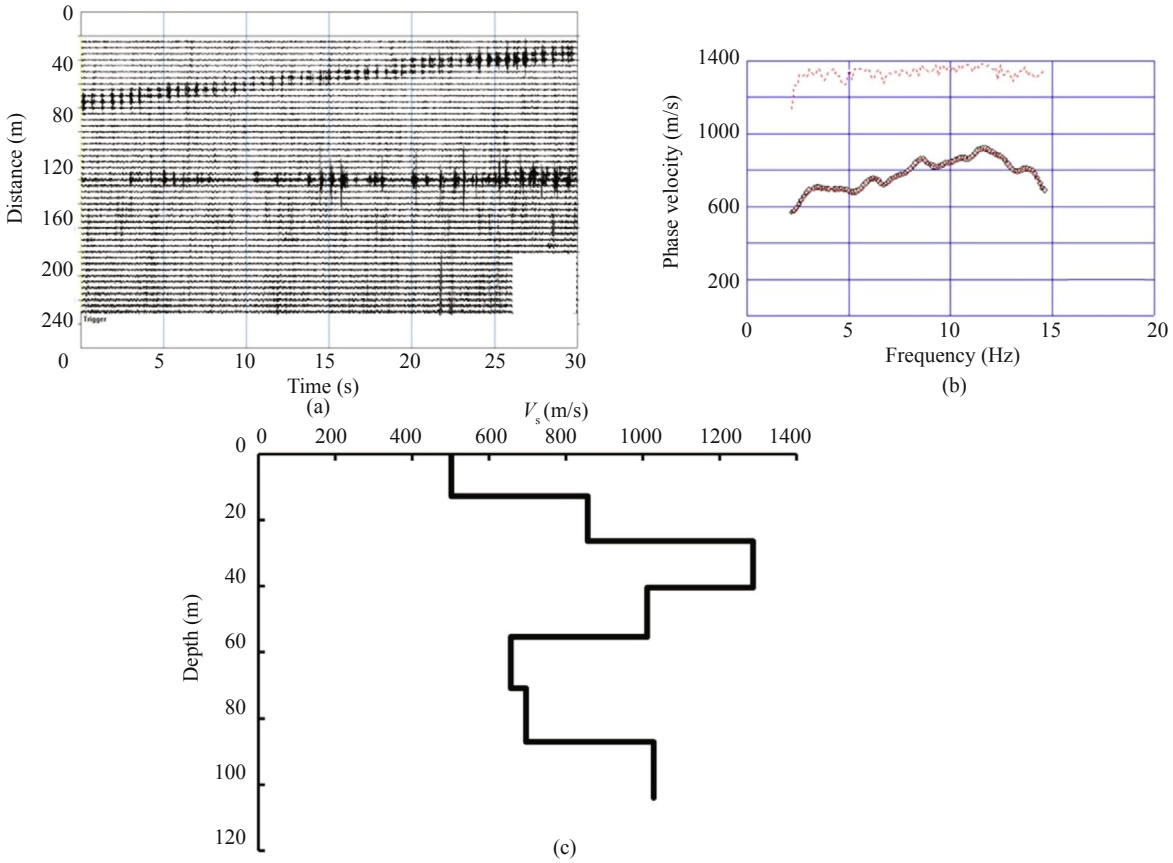

Fig. 6 Data processing steps of ReMi data in Site P: (a) An example of ReMi records; (b) Determining the phase velocity of each frequency (Dotted red line shows that signal/noise ratio, Continuous red line shows that determined fundamental mode dispersion curve); (c) Shear wave velocity (V_s) profile

a pass band-pass of 0.05–20 Hz. Then they were divided into 25 s long windows and tapered individually using the Konno-Ohmachi smoothing method. For each window, the amplitude spectra of the three components were computed using a Fast Fourier Transform (FFT) algorithm. As a result, the average spectral ratio of horizontal-to-vertical noise components was thus calculated. Microtremor measurements were processed using the GEOPSY software package (www.geopsy.org).

Figure 7 shows the data-processing steps taken at the B1 microtremor measurement site. Two peaks are noteworthy in the obtained *H/V* spectral ratio (Fig. 8); the first occurred at very low frequencies (0.2–0.8 Hz), whereas the other changed from 4 to 20 Hz. Although very low frequencies are often not considered in engineering studies, *H/V* curves are directly involved in the interface characteristics (i.e., depth and impedance contrast) of bedrock and sediment units, and the first peak was associated with impedance contrast (V_s > 3000 m/s).

SPAC measurements were taken at each site using circular array CMG-6TD three-component seismometers, which consist of three recording stations on the ring and another in the center. The radii of the circular arrays were individually adjusted for each site in the range of 20–227 m (P1: r1,2,3 = 25, 90, and 227 m; P8: r1,2,3 = 20, 75, and 198 m; P3: r1,2,3 = 30, 60, and 90 m; P12: r1,2,3 = 30, 60, and 100 m), and recording duration changed from 30 to 60 min at each array. SPAC coefficients obtained from observed values and theoretical Bessel function values were investigated

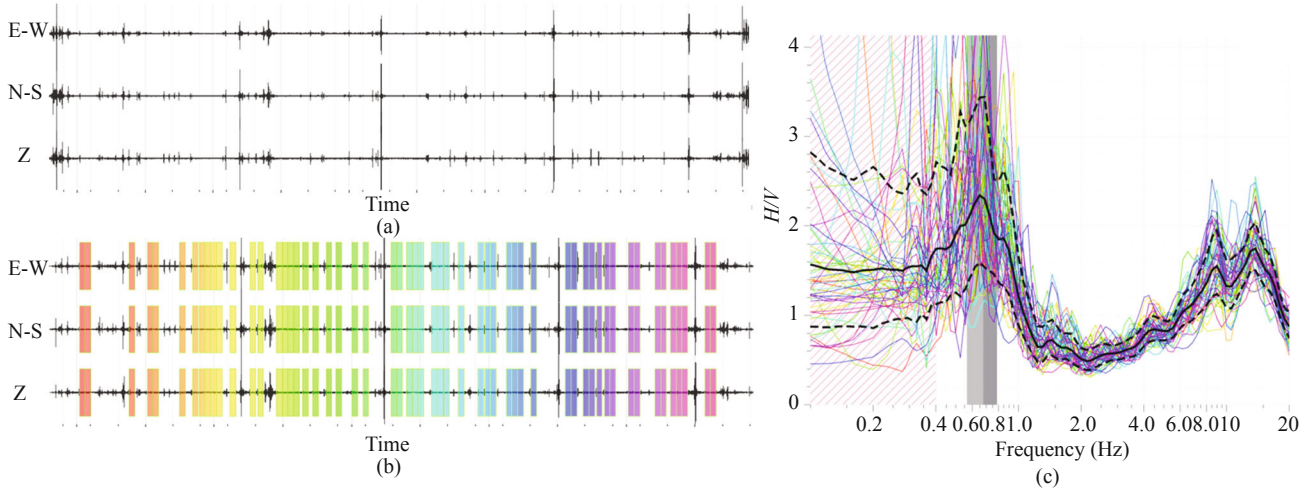

Fig. 7 Data processing steps for B1 microtremor measurement site: (a) Three-component records; (b) Windowing with 25 s; (c) *H/V* spectral ratio

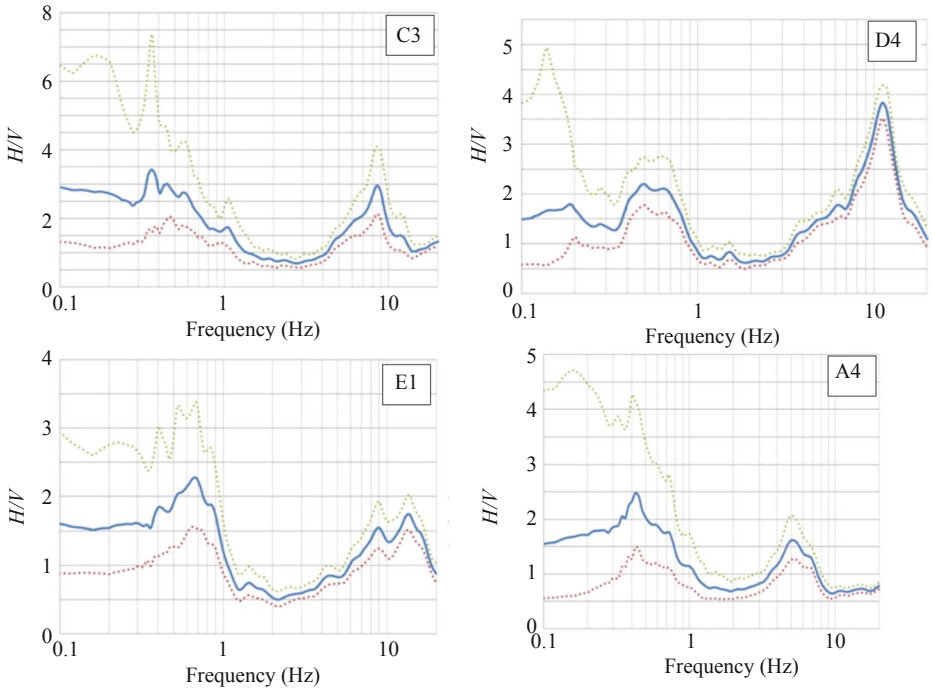

Fig. 8 Examples of *H/V* spectral ratio for study area (dashed lines demonstrates the standard deviation)

by computing the dispersion curve values of the corresponding frequency range. After obtaining the dispersion curves, one-dimensional *S*-wave velocities were obtained by applying the least-squares method (Levenberg, 1944; Marquardt, 1963). Dispersion curves obtained by active (i.e., MASW) and passive (i.e., ReMi and SPAC) surface wave methods were combined to enlarge the analyzable frequency range of dispersion and improve the modal identity of the dispersion trends (Fig. 9). High-resolution V_s profiles were obtained by inverting the dispersion curve, and S-wave velocities were obtained from the combined dispersion curves using the damped least-squares method (Figs. 10, 11 and 12).

The Earthquake Research and Implementation Center at Dokuz Eylül University performed drilling and MASW measurements near the borehole within the scope of TUBITAK-KAMAG (Project No. 106G159) in 2008. According to the drilling report, the ground is gravelly clay at a depth down to 1.4 m, at which point the ground becomes clayey limestone until a depth of 20 m (Fig. 13(a)). However, the clayey limestone is not homogeneous, meaning that the geological unit's V_s values differ by depth.

As seen in the Fig. 13(b), although clayey soil is dominant in 20-160 m depth, higher than 760 m/s velocity values have been observed in V_s sections that are compatible with the first 180 m of V_s- depth section at P8 site obtained as a result of inversion of combined dispersion curves and DRL 2 drilling log implemented as part of water studies of study area in 2002. It is interpreted that these high velocities were caused by gravel and block limestones in the clayey unit observed in the drilling log.

A V_{s30} contour map beginning with the V_s depth section obtained from the combined dispersion of ReMi and MASW was constructed; the V_{s30} values varied between 420 and 960 m/s (Table 1). Whereas the velocities decreased in the southwest part of the study area, high velocities were observable in the northern parts (Fig. 14). According to the National Earthquake Hazards Reduction Program's (NEHRP) (1997) soil classification system based on V_{s30} values, which are critical parameters in the geotechnical analysis, the study area was mostly of NEHRP Classes B and C (Table 1).

Engineering bedrock ($V_s > 760$ m/s) depth in the study area was three-dimensionally mapped with topography (Fig. 15 and Table 1) and its maximum depth was

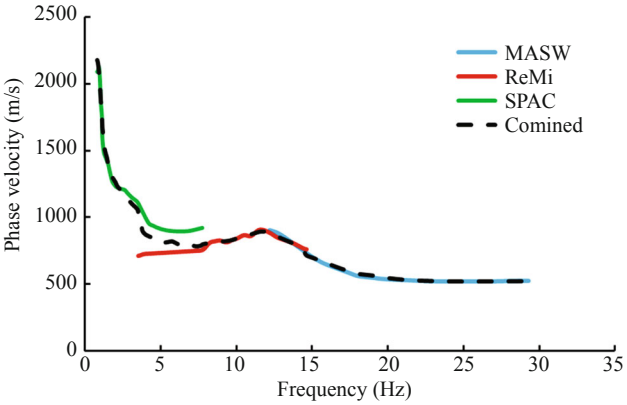

Fig. 9 An example of combining dispersion curves of Rayleigh waves determined by the all surface wave methods at Site P1

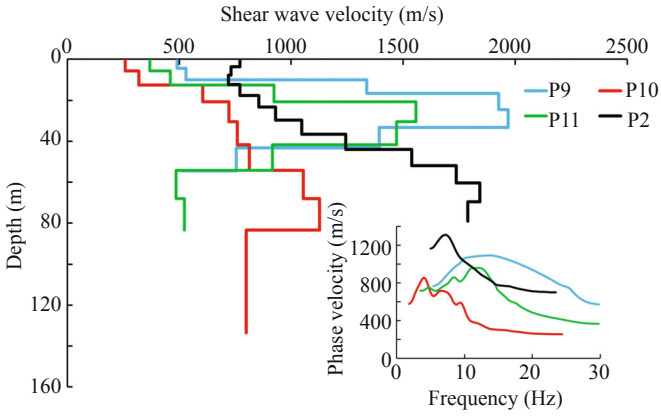

Fig. 10 (a) Dispersion curves of Rayleigh waves at Sites P2, P9, P10 and P11; (b) Shear wave velocities were obtained from the combined dispersion curves

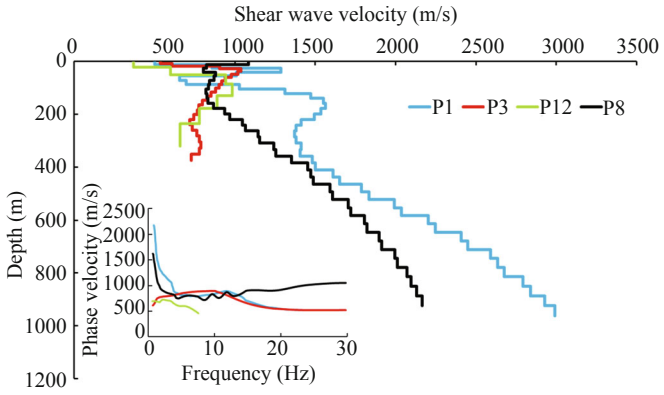

Fig. 11 (a) Dispersion curves of Rayleigh waves at Sites P1, P3, P8 and P12; (b) Shear wave velocities were obtained from the combined dispersion curves

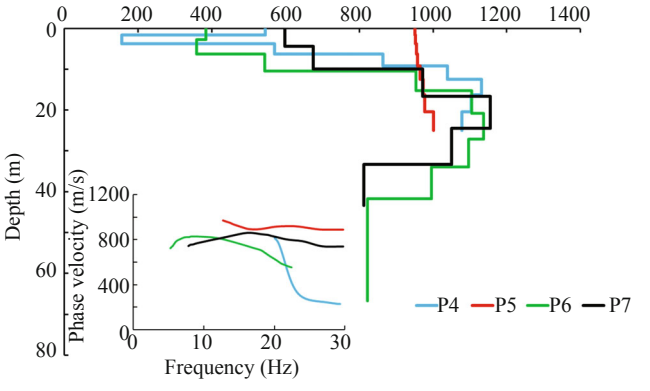

Fig. 12 (a) Dispersion curves of Rayleigh waves at Sites P4, P5, P6 and P7; (b) Shear wave velocities were obtained from the combined dispersion curves

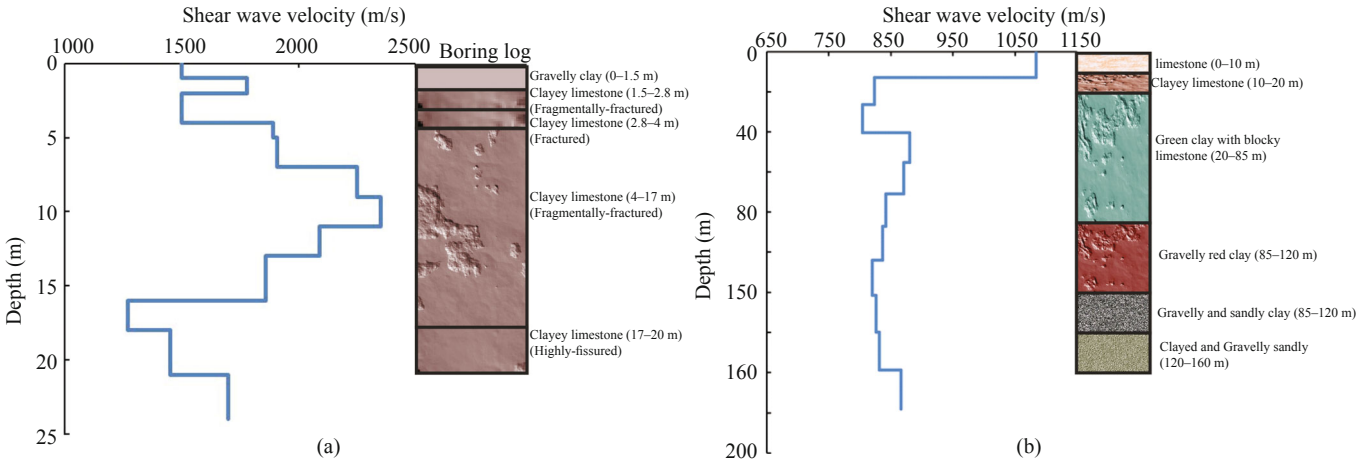

Fig. 13 (a) Shear wave velocity (MASW) section and the borehole at DRL, (b) Shear wave velocity (Part of P8 Site) section and the borehole at DRL 2

Table 1 V_{s30} Values, estimated engineering bedrock depths, Z1.0 depth and soil class for study area

V_s measurement sites	X (UTM-WGS84)	Y (UTM-WGS84)	AV_s30 (m/s)	Engineering bedrock depth (m)	Z1.0 depth (m)	Soil class (NEHRP, 1997)
P1	518322	4246453	687	12	26.3	C
P2	518020	4246367	796	0	29.67	B
P3	518072	4246746	966	17.39	27.17	B
P4	517888	4246816	644	6.25	9.16	C
P5	518378	4246735	700	0	20.42	C
P6	517587	4247031	780	10.42	15.27	B
P7	517611	4246897	858	10	16.66	B
P8	517326	4247154	850	0	0	B
P9	517415	4246884	851	10	10	B
P10	517588	4246530	430	30.55	54.16	C
P11	518091	4246628	680	12.5	20.83	C

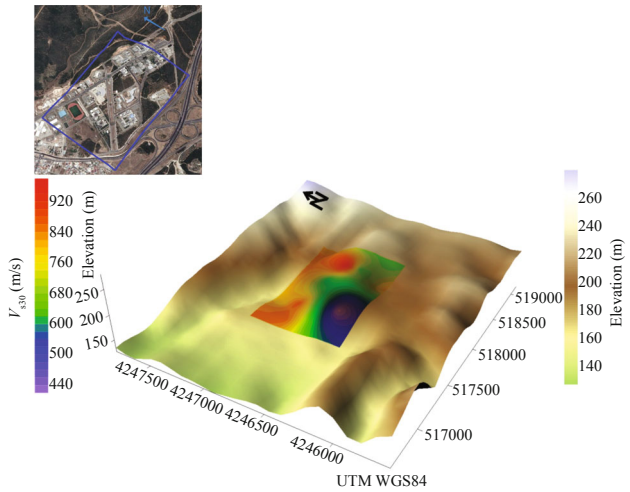

Fig. 14 V_{s30} contour map of the study area

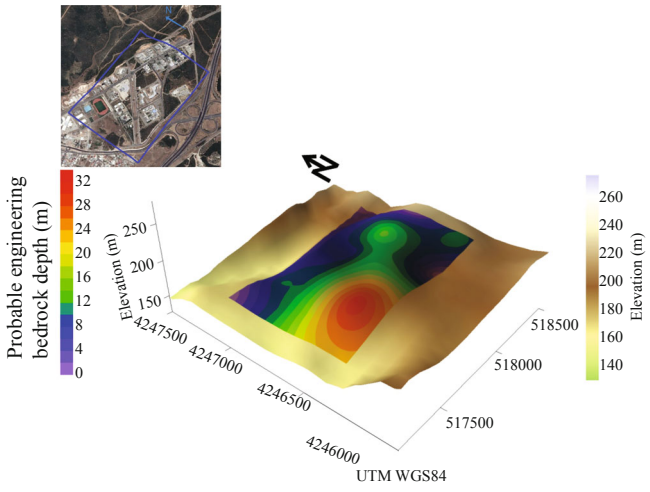

Fig. 15 Probable engineering bedrock mapping (3D)

determined to be 30 m. In the northeast and northwest parts of the study area, the depth was approximately 5 m, yet it reached 30 m in the southwest due to increased sediment unit thickness. As shown in Table 1, the Z1.0 parameter (i.e., depth of horizon layers of V_s = 1000 m/s) now often used in ground motion prediction equations was determined (Chiou and Youngs, 2008, 2014).

In addition, the predominant periods, depending on local soil conditions of ground motion, were determined by using the single station microtremor (i.e., Nakamura's) method (Table 2). Figure 16 shows the predominant period contour map of the area and that predominant period values ranged from 0.05 to 0.2 s. Given the possibility of inferring a relationship between V_{s30} and T_0 (Castellaro *et al*., 2008; Kuo *et al*., 2015), the V_{s30} map and the dominant period map are arguably compatible. A comparison of T_0 and V_{s30} values obtained showed a good correlation characterized by a linear trend in Tınaztepe (Fig. 17). A linear regression on the data was then performed and a result of V_{s30} = $-3{,}262.7T_0 + 1{,}122.5$ was obtained, in which T_0 is the predominant period with a determination coefficient of 0.72. Where velocities were high, the periods were low; where the velocities were low, the periods were high.

Regarding changes of the dominant period, V_{s30} and topography were examined in the A-A' section, which showed S-wave velocity sections obtained from combined dispersion curves at sites P1, P3, and P8. As Fig. 18 shows, V_{s30} values gradually increased toward to east, whereas predominant periods decreased (Fig. 18).

Table 2 Predominant Period Values

Microtremor station	X (UTM-WGS84)	Y (UTM-WGS84)	Predominant period (s)
A1	517450	4247050	0.07
A2	517418	4246870	0.07
A3	517350	4246715	0.06
A4	517304	4246582	0.20
B1	517720	4247140	0.11
B2	517627	4246930	0.11
B3	517535	4246698	0.17
B4	517464	4246456	0.20
C1	518035	4247035	0.14
C2	517955	4246852	0.14
C3	517830	4246627	0.14
C4	517743	4246420	0.15
D1	518296	4246919	0.09
D2	518213	4246720	0.14
D3	518118	4246508	0.10
D4	518038	4246354	0.10
E1	518729	4246788	0.11
E2	518554	4246646	0.13
E3	518384	4246493	0.17
E4	518211	4246349	0.19
F1	518320	4246757	0.10
F2	518085	4246860	0.07
F3	517850	4246954	0.14
F4	517592	4247041	0.14
F5	517392	4247128	0.16
G1	517190	4247224	0.10
G2	517104	4247177	0.09
G3	516999	4247122	0.09

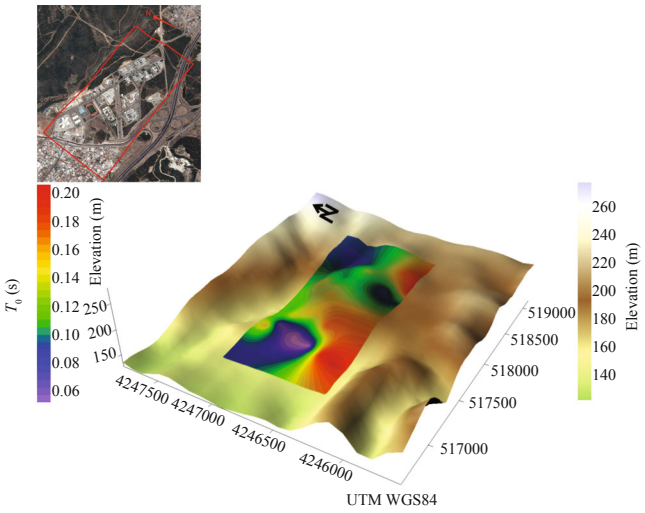

Fig. 16 Predominant period contour map of the study area

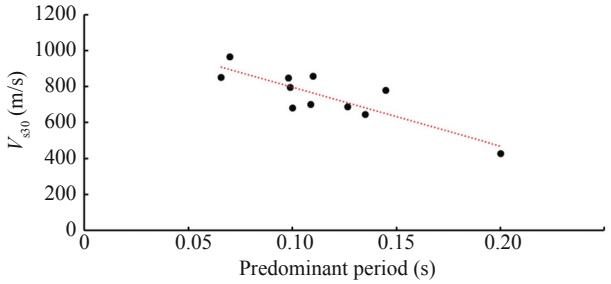

Fig. 17 Correlation between V_{s30} and predominant period. A linear regression resulted in equation V_{s30}=-3262.7T_0+ 1122.5 plotted as a red line with R^2 = 0.72

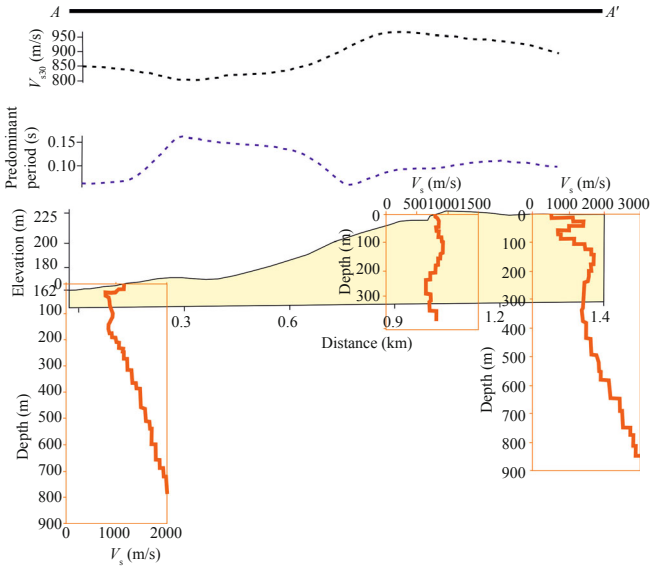

Fig. 18 Changes of V_{s30}, predominant period and topography in *A*-*A*′ section

5 Conclusions

The S-wave velocity and soil stratification were determined by using surface wave methods (i.e., MASW, ReMi, and SPAC) that use the dispersive curve of Rayleigh waves. SPAC measurements were used to obtain V_s in deeper sections, whereas MASW and ReMi were used to find V_s from shallower ones. Dispersion curves obtained with the methods were then combined to obtain high-resolution V_s profiles.

Single station microtremor measurements were performed at 28 sites, and using the horizontal-to-vertical spectral ratio (HVSR), the predominant period and *H*/*V* spectral ratio were identified at each site. Since the distribution of predominant periods correlates with the geology and other geophysical methods in the study area, the site classification map derived for this study was based only on the predominant period distribution map. Our analysis of single station microtremor measurements showed that resonance frequency does not vary considerably throughout Tınaztepe, since it decreases when basement depth increases. The results of microtremor data also conform with S-wave velocity profiles in the study area.

It was specified that the engineering bedrock was no deeper than 30 m and that the S-wave velocity in the ground would not change suddenly in the lateral and vertical directions in Tınaztepe. When compared, the depth of engineering bedrock and the dominant period map are generally compatible. Particularly in the southeast section of the study area, the increased depth of bedrock and values increases in the dominant period are remarkable. Regression results (V_{s30} = -3262.7T_0 + 1122.5) thus provided an efficient assessment tool for V_{s30}, though the data show obvious scattering.

An analysis of deep S-wave velocity sections obtained with SPAC indicates that velocities generally increase in parallel with depth; however, at some depths, they decrease due to possible fractured-fissured structures in geological units. As the analysis of the boreholes in the study area and the adjoining S-wave velocity section obtained by MASW showed, velocity changes at less than 15 m arise from the fissured structure in the unit, not from geological unit differences. Since the depth of the engineering bedrock was no deeper than 30 m, NEHRP soil classes were available and the soil type of the study area was found to be of class B and C according to the V_{s30} values (Table 1).

According to Özdağ (*et al*., 2015), the Bornova Complex unit was defined as engineering bedrock surrounding İzmir Bay has not been observed after DRL boring at 25 m depth and DRL 2 boring at 180 m depth. In addition, the state of V_s >760 m/s (engineering bedrock) has been reached in the first 30 m. Due to these reasons, for the soil stratification at the depth where it

shows engineering bedrock properties for the study area, it has not been possible to designate a generalized geological denomination.

For the study area, the ground shows acoustic impedance changes in the lateral and vertical direction. This situation reveals that a homogeneous effect on the ground surface in the event of a possible earthquake affecting the study area should not be expected. It is suggested that these effects for the study area be studied via 2D and 3D modeling.

Acknowledgement

This work was performed within part of Mr. Eren Pamuk's master thesis at Dokuz Eylul University, The Graduate School of Natural and Applied Sciences. The borilling report and the MASW measurement (near the borehole) in this research were provided by TUBITAK-KAMAG (Project No. 106G159). GMT (Wessel and Smith, 1995) was used to create Figure 2. The authors also thank the anonymous reviewers for their helpful comments.

References

Akgün M Gönenç T Pamukçu O Özyalın Ş and Özdağ ÖC (2013), "Integrated Geophysical Methods for the Determination of Engineering Bedrock: İzmir New City Center," *Jeofizik*, **18**: 67–80. (in Turkish)

Aki K (1957), "Space and Time Spectra of Stationary Stochastic Waves, with Special Reference to Microtremors," *Bulletin of the Earthquake Research Institute*, **35**: 415–456.

Akkaya İ (2015), "The Application of HVSR Microtremor Survey Method in Yüksekova (Hakkari) Region, Eastern Turkey," *Journal of African Earth Sciences*, **109**: 87–95

Anbazhagan P and Sitharam TG (2009), "Spatial Variability of the Depth of Weathered and Engineering Bedrock Using Multichannel Analysis of Surface Wave Method," *Pure and Applied Geophysics*, **166**(3): 409–428.

Asten WM (2006), "On Bias and Noise in Passive Seismic Data from Finite Circular Array Data Processed Using SPAC Methods," *Geophysics*, **71**(6) :153–162.

Bard PY (1998), "Microtremor Measurements: A Tool for Site Effect Estimation," *Proceedings of 2nd International Symposium on the Effect of Surface Geology on Seismic Motion*, Vol III, Yokohama, Japan, pp. 1251–1279.

Bettig B Bard PY Scherbaum F Riepl J and Cotton F (2001), "Analysis of Dense Array Noise Measurements Using the Modified Spatial Auto-correlation (SPAC)-Application to Grenoble Area," *Bolletino di Geofisica Teorica ed Applicata,* **42**: 281–304.

Castellaro S Mulargia F and Rossi PL (2008),"V_{s30}: Proxy for Seismic Amplification?" *Seismol. Res. Lett.*, **79**: 540–543.

Chavez-Garcia FJ Rodriguez M and Stephenson WR (2005), "An Alternative Approach to the SPAC Analysis of Microtremors: Exploiting Stationarity of Noise," *Bulletin of the Seismological Society of America*, **95**: 277–293.

Chavez-Garcia FJ Rodriguez M and Stephenson WR (2006), Subsoil Structure Using SPAC Measurements along a Line, *Bulletin of the Seismological Society of America*, **96**: 729–736.

Chiou BSJ and Youngs RR (2008)," An NGA Model for the Average Horizontal Component of Peak Ground and Response Spectra," *Earthquake Spectra*, **24**(1): 173–215.

Chiou BSJ and Youngs RR (2014), "Update of the Chiou and Youngs NGA Model for the Average Horizontal Component of Peak Ground Motion and Response Spectra," *Earthquake Spectra*, **30**(3): 1117–1153.

Code TE (2007), *Specification for Structures to be Built in Disaster Areas*, Ministry of Public Works and Settlement Government of Republic of Turkey.

Dikmen Ü and Mirzaoğlu M (2005), "The Seismic Microzonation Map of Yenisehir-Bursa, NW of Turkey by Means of Ambient Noise Measurements," *Balkan Geophysics Society*, **8**(2): 53–62.

EC8 (2004), *Eurocode 8: Design of Structures for Earthquake Resistance. Part 1: General Rules, Seismic Actions and Rules for Buildings*, European Norm, European Committee for Standardisation, European Committee for Standardisation Central Secretariat, Rue de Stassart 36, B-1050 Brussels, Belgium

Gitterman Y Zaslavsky Y Shapira A and Shtivelman V (1996)," Empirical Site Response Evaluations: Case Studies in Israel," *Soil Dynamic Earthquake Engineering*, **15**: 447–463.

Groundwater Study of Report (2002), Dokuz Eylül University.

Kanlı Aİ, Tildy P, Pronay Z, Pınar A and Hemann L (2006), "V_{s30} Mapping and Soil Classification for Seismic Site Effect Evaluation in Dinar Region, S_w Turkey," *Geophysical Journal International*, **165**: 223–235.

KOERI (2015), Bogazici University Kandilli Observatory and Earthquake Research Institute Regional Earthquake-Tsunami Monitoring Center (KOERI) website. [Online]. Available: http://www.koeri.boun.edu.tr/sismo/2/en/

Konno K and Ohmachi T (1998), "Ground-motion Characteristics Estimated from Spectral Ratio between Horizontal and Vertical Components of Microtremor, *Bulletin of the Seismological Society of America*, **88**: 228–241.

Köhler A Ohrnberger M Scherbaum F Wathlet M and Cornou C (2007), Assessing the Reliability of the

Modified Three-component Spatial Autocorrelation Technique, *Geophysical Journal International,* **168**: 779–796.

Kuo CH Wen KL Lin CM Wen S and Huang JY (2015), "Investigating Near Surface Swave Velocity Properties Using Ambient Noise in Southwestern Taiwan," *Terr. Atmos. Ocean. Sci*., **26**: 205–211.

Lachet C and Bard PY (1994), "Numerical and Theoretical Investigations on the Possibilities and Limitations of Nakamura's Technique," *Journal of Physics of the Earth*, **42**(5): 377–397.

Lermo J and Chavez-Garcia FJ (1993), "Site Effect Evaluation Using Spectral Ratios with Only One Station," *Bulletin of the Seismological Society* of America, **83**: 1574–1594.

Lermo J and Chavez-Garcia FJ (1994), "Are Microtremors Useful in Site Response Evaluation?," *Bulletin of the Seismological Society of America*, **84**: 1350–1364.

Levenberg K (1944), "A Method for the Solution of Certain Non-linear Problems in Least Squares" *Quarterly of Applied Mathematics*, **2**: 164–168.

Liu HP Boore DM Joyner WB Oppenheimer DH Warrick RE Zhang W Hamilton JC and Brown LT (2000), "Comparison of Phase Velocities from Array Measurements of Rayleigh Waves Associated with microtremors and Results Calculated from Borehole Shear-wave Velocity Profiles," *Bulletin of The Seismological Society of America*, **90**: 666–678.

Louie JN (2001), "Faster, Better: Shear-wave Velocity to 100 Meters Depth from Refraction Microtremor Arrays," *Bulletin of the Seismological Society of America*, 91: 347–364.

Marquardt D (1963), "An Algorithm for Least-squares Estimation of Nonlinear Parameters," *Journal of the Society for Industrial and Applied Mathematics*, **11**(2): 431–441.

Morikawa H Sawada S and Akamatsu J (2004), "A Method to Estimate Phase Velocities of Rayleigh Waves Using Microtremors Simultaneously Observed at Two Sites," *Bulletin of the Seismological Society of America*, 94: 961-976.

Mucciarelli M (1998), "Reliability and Applicability of Nakamura's Technique Using Microtremors: An Experimental Approach," *Journal of Earthquake Engineering*, 4: 625–638.

Nakamura Y (1989), "A Method for Dynamic Characteristics Estimation of Sub-surface Using Microtremor on the Ground Surface," *Quarterly Report of Railway Technical Research Institute*, 30: 25-33.

NEHRP (1997), "Recommended Provisions For Seismic Regulations For New Buildings and Other Structures, FEMA-303," Prepared by the Building Seismic Safety Council for the Federal Emergency Management Agency, Washington, DC.

Nogoshi M and Igarashi T (1970), "On The Propagation Characteristics of Microtremor," *Journal of the Seismological Society of Japan*,23: 264–280.

Ohori M Nobata A and Wakamatsu K (2002), "A Comparison of ESAC and FK Methods of Estmating Phase Velocity Using Arbitrarily Shaped Microtremor Arrays," *Bulletin of the Seismological Society of America*, **92**: 2323–2332.

Okada H (2003), "The Microtremor Survey Method," *Geophysical Monograph*, No. 12, Society of Exploration Geophysicists, Tulsa.

Özdağ ÖC, Gönenç T and Akgün M (2015), "Dynamic Amplification Factor Concept of Soil Layers: A Case Study in İzmir (Western Anatolia)," *Arabian Journal of Geosciences*, **8**(11): 10093–10104.

Pamuk E Özyalin S Akgün M and Özdag CÖ (2014), "An Integrated Interpretation of Combining Dispersion Curves Obtained by Using Active & Passive Source Methods and Calculated *S*-wave Velocity Profiles: A Case Study of Izmir/Turkey," *In EGU General Assembly Conference Abstracts*, **16**: 710–710.

Park CB and Miller RD (2005), "Seismic Characterization of Wind Turbine Sites in Kansas by the MASW Method," *Kansas Geological Survey Open-file Report*, 2005-23.

Park CB Miller RD and Xia J (1999), "Multichannel analysis of Surface Waves," *Geophysics, 64*:800-808.

Tokimatsu K Tamura S and Kojima K (1992), "Effects of Multiple Mode on Rayleigh Wave Dispersion Characteristics," *Journal of Geotechnical Engineering*, **118**: 1529–1543.

Uzel B, Sözbilir H and Özkaymak Ç (2012), "Neotectonic Evolution of an Actively Growing Superimposed Basin in Western Anatolia: The Inner Bay of İzmir, Turkey," *Turkish Journal of Earth Sciences*, **21**(4): 439–471.